PHYSICAL REVIEW A **92**, 052124 (2015)

General description of quasiadiabatic dynamical phenomena near exceptional points

Thomas J. Milburn,[1,*] Jörg Doppler,[2] Catherine A. Holmes,[3] Stefano Portolan,[4] Stefan Rotter,[2] and Peter Rabl[1]
[1]*Institute of Atomic and Subatomic Physics, Vienna University of Technology, Stadionallee 2, 1020 Vienna, Austria*
[2]*Institute for Theoretical Physics, Vienna University of Technology, 1040 Vienna, Austria*
[3]*School of Mathematics and Physics, University of Queensland, St. Lucia, Queensland 4072, Australia*
[4]*Department of Physics and Astronomy, University of Southampton, Southampton SO17 1BJ, United Kingdom*
(Received 8 June 2015; published 30 November 2015)

The appearance of so-called exceptional points in the complex spectra of non-Hermitian systems is often associated with phenomena that contradict our physical intuition. One example of particular interest is the state-exchange process predicted for an adiabatic encircling of an exceptional point. In this work we analyze this and related processes for the generic system of two coupled oscillator modes with loss or gain. We identify a characteristic system evolution consisting of periods of quasistationarity interrupted by abrupt nonadiabatic transitions and we present a qualitative and quantitative description of this switching behavior by connecting the problem to the phenomenon of stability loss delay. This approach makes accurate predictions for the breakdown of the adiabatic theorem as well as the occurrence of chiral behavior observed previously in this context and provides a general framework to model and understand quasiadiabatic dynamical effects in non-Hermitian systems.

DOI: 10.1103/PhysRevA.92.052124 PACS number(s): 03.65.Ca, 42.25.−p, 42.55.−f

I. INTRODUCTION

The quantum adiabatic theorem is a seminal result in the history of quantum mechanics. Paraphrasing Born, the theorem states that for an infinitely slow parametric perturbation there is no possibility of a quantum jump [1]. Many physical phenomena observed in both quantum and classical systems can be explained by this theorem, ranging from optical tapers [2] to robust quantum gates [3]. Recently, the applicability of adiabatic principles to non-Hermitian systems, e.g., coupled harmonic modes with gain or loss, has attracted considerable attention. Here the complex eigenvalue structure and the existence of so-called exceptional points (EPs) leads to new counterintuitive phenomena [4–18]. Perhaps most strikingly, adiabatically encircling an EP was predicted to effect a state exchange, with applications for switching and cooling [19–21]. However, it is now known that the very presence of non-Hermiticity prevents a general application of the adiabatic theorem [22–24] and the inevitability of nonadiabatic transitions leads to new effects, e.g., to chiral behavior [25–30].

Whereas the above results point to fascinating new physical phenomena, the complexity of the problem mostly requires one to resort to numerical studies (as cited above) or to focus on limiting cases where the system evolution is eventually dominated by a single mode with maximum gain or minimum loss. An important step beyond this limitation has been presented in Refs. [26,31], in which an exactly solvable model is considered and a connection between the appearance of nonadiabatic transitions and the Stokes phenomenon of asymptotics [32] is thereby found. However, even for very simple scenarios, these exact case studies are mathematically already quite involved and the translation of the observed dynamics to other systems, in particular to realistic systems with imperfections and noise, is not immediately obvious.

In this work we analyze quasiadiabatic dynamics in non-Hermitian systems near EPs with the aim to provide a generalized framework for both modeling and understanding the associated dynamical phenomena. Our approach reveals that the solutions are in general composed of periods of quasistationary evolution during which the solution follows fixed points, interrupted by abrupt nonadiabatic transitions due to the exchange of stability. However, the time of these transitions cannot be predicted by a standard stability analysis and, intriguingly, we find that piecewise adiabaticity is still a key ingredient for understanding the evolution of the system in spite of an overall breakdown of adiabatic principles.

On a more fundamental level, our analysis shows that the quasiadiabatic dynamics near an EP is a singularly perturbed problem [33], meaning that, in contrast to Hermitian systems, the dynamics cannot be obtained by perturbative corrections to the adiabatic prediction. This fact makes adiabatic principles in non-Hermitian systems particularly interesting as well as challenging to understand, both from a physical and from a mathematical point of view. Specifically, here we connect the problem of nonadiabatic transitions to the more general phenomenon of stability loss delay [34,35] in dynamical bifurcations. This concept more easily affords intuition in complicated examples where exact solutions cannot be found and in realistic systems where noise cannot be ignored. Our results are therefore important for a variety of modern-day experiments with, e.g., waveguides [15,16], coupled resonators [17,18], semiconductor microcavities [36], or electromechanical [37,38] and optomechanical systems [39–41], which offer sufficiently high control for the observation of the predicted dynamical phenomena.

II. NON-HERMITIAN DYNAMICS AND EXCEPTIONAL POINTS

A. Model

For the following discussion we consider the generic model of two coupled harmonic oscillators with frequencies ω_1 and ω_2, decay rates γ_1 and γ_2, and coupling strength g [see Fig. 1(a)]. The equations of motion for the amplitudes α_1 and

*thomas.milburn@ati.ac.at

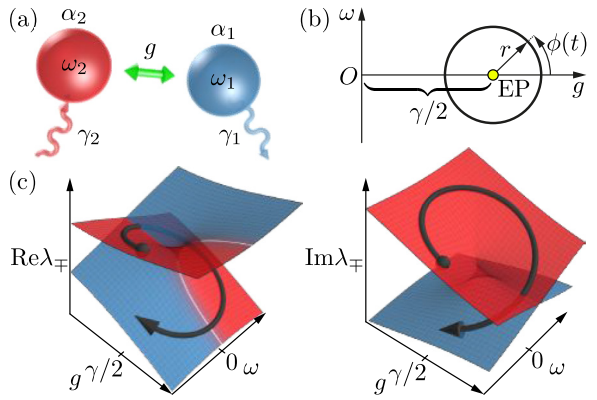

FIG. 1. (Color online) (a) Cartoon of two coupled harmonic modes with gain or loss. (b) Example of a parametric path where γ is fixed, $\omega = r\sin\phi(t)$, and $g = \gamma/2 + r\cos\phi(t)$. (c) Real (Re) and imaginary (Im) parts of the spectrum $\lambda_\mp = \mp\sqrt{(\omega + i\gamma/2)^2 + g^2}$. The curve is the trajectory of λ_- for the path defined in (b) and depicts the fully adiabatic evolution.

α_2 are

$$\frac{d}{dt}\begin{pmatrix}\alpha_1\\ \alpha_2\end{pmatrix} = -i\begin{pmatrix}\omega_1 - i\gamma_1/2 & g\\ g & \omega_2 - i\gamma_2/2\end{pmatrix}\begin{pmatrix}\alpha_1\\ \alpha_2\end{pmatrix}, \quad (1)$$

where in general $\omega_i = \omega_i(t)$, $\gamma_i = \gamma_i(t)$, and $g = g(t)$ are functions of time. For the following analysis it is convenient to eliminate the common evolution with average frequency $\Omega := (\omega_2 + \omega_1)/2$ and average decay rate $\Gamma := (\gamma_2 + \gamma_1)/2$ by introducing a new set of amplitudes β_1 and β_2 via

$$\begin{pmatrix}\alpha_1(t)\\ \alpha_2(t)\end{pmatrix} = \exp\left(-i\int^t [\Omega(t') - i\Gamma(t')/2]dt'\right)\begin{pmatrix}\beta_1(t)\\ \beta_2(t)\end{pmatrix}. \quad (2)$$

The remaining nontrivial dynamics in this frame is

$$\frac{d}{dt}\begin{pmatrix}\beta_1\\ \beta_2\end{pmatrix} = -i\begin{pmatrix}-\omega - i\gamma/2 & g\\ g & \omega + i\gamma/2\end{pmatrix}\begin{pmatrix}\beta_1\\ \beta_2\end{pmatrix}, \quad (3)$$

where $\omega := (\omega_2 - \omega_1)/2$ and $\gamma := (\gamma_1 - \gamma_2)/2$. Note that while the global transformation (2) does not affect any of the following results, if $\Gamma \neq 0$ then the experimentally observable amplitudes $\alpha_{1,2}$ are related to $\beta_{1,2}$ by an exponentially large or small prefactor.

Below we suppose that at least ω and g, or ω and γ, can be controlled as a function of time. This can be achieved, e.g., with optical modes propagating through waveguides with spatially varying losses [42,43], by applying chirped laser pulses to molecular systems [27], or by using two mechanical resonators with electrically [37,38] or optomechanically [39–41] controlled parameters.

B. Exceptional points

Let us write Eq. (3) more compactly as $\dot{\vec{x}} = -i\mathbf{M}\vec{x}$, where $\vec{x}$ is the state vector and $\mathbf{M}$ is the dynamical matrix, or sometimes called in this context a non-Hermitian Hamiltonian [9], i.e.,

$$\vec{x} := \begin{pmatrix}\alpha_1\\ \alpha_2\end{pmatrix}, \quad \mathbf{M} := \begin{pmatrix}-\omega - i\gamma/2 & g\\ g & \omega + i\gamma/2\end{pmatrix}. \quad (4)$$

Here $\mathbf{M}$ has eigenvalues $\lambda_\mp = \mp\lambda = \mp\sqrt{(\omega + i\gamma/2)^2 + g^2}$. Since $\mathbf{M}$ is non-Hermitian, it does not have an orthonormal eigenbasis in the sense of Dirac, but rather a biorthogonal eigenbasis with right eigenvectors $\vec{r}_\mp$ defined via $\mathbf{M}\vec{r}_\mp = \lambda_\mp\vec{r}_\mp$ and left eigenvectors $\vec{l}_\mp$ defined via $\vec{l}_\mp^{\,T}\mathbf{M} = \vec{l}_\mp^{\,T}\lambda_\mp$ such that $\vec{l}_i^{\,T}\vec{r}_j = \delta_{i,j}$. One has some freedom in choosing the eigenbasis, but a pertinent choice is the parallel transported eigenbasis

$$\vec{r}_- = \vec{l}_- = \begin{pmatrix}\cos\vartheta/2\\ \sin\vartheta/2\end{pmatrix}, \quad \vec{r}_+ = \vec{l}_+ = \begin{pmatrix}-\sin\vartheta/2\\ \cos\vartheta/2\end{pmatrix}, \quad (5)$$

with ϑ such that $\tan\vartheta = -g/(\omega + i\gamma/2)$ (see Appendix A 1 for more details). Figure 1(c) shows the real (Re) and imaginary (Im) parts of $\lambda_\pm$ as a function of g and ω with γ fixed. The pinch points $\omega + i\gamma/2 \mp ig = 0$ are EPs [4–10]. At these points the eigenvalues and the eigenvectors coalesce and $\mathbf{M}$ becomes nondiagonalizable. Encircling an EP with a closed path in parameter space causes the two eigenvalues, and hence also the two eigenvectors, to swap [see Figs. 1(b) and 1(c)]. Based on intuition from the quantum adiabatic theorem, it was suggested that this unique feature could be observed in physical systems by encircling an EP over a time T such that $T|\lambda_- - \lambda_+|$ is large [19–21]. However, other studies contradict this result and show that due to non-Hermiticity this picture cannot hold in general [22–30].

C. Numerical examples

Before presenting a further analytic treatment of Eq. (3), we consider in Fig. 2 some typical solutions for encircling an EP with $T|\lambda_- - \lambda_+| \gg 1$. For these examples we choose a path in parameter space as defined in Fig. 1(b). We expand the solution as

$$\vec{x}(t) = c_-(t)\vec{r}_-(t) + c_+(t)\vec{r}_+(t), \quad (6)$$

where $\vec{r}_-(t)$ and $\vec{r}_+(t)$ are the instantaneous eigenvectors of $\mathbf{M}(t)$, and we choose the initial condition $c_-(0) = 1$ and $c_+(0) = 0$. One may reconstruct the amplitudes $c_\mp(t)$ from a solution $\vec{x}(t)$ via $c_\mp(t) = \vec{l}_\mp^{\,T}(t)x(t)$. The adiabatic prediction is $c_-^{\mathrm{ad}}(t) \simeq \exp[-i\int_0^t \lambda_-(t')dt']$ and $c_+^{\mathrm{ad}}(t) \ll c_-^{\mathrm{ad}}(t)$. Since we have chosen a parallel transported eigenbasis, no geometric phase appears in the evolution of the amplitudes $c_\mp$. This makes evaluating adiabaticity much simpler [44]. Furthermore, as discussed in Ref. [45], the populations $|c_\mp(t)|^2$ more closely match physical populations than other conventions because their evolution includes the dynamical phase, which for a non-Hermitian system contains gain or loss effects.

In examples (i) and (ii) in Fig. 2 we have chosen a counterclockwise and a clockwise encircling, respectively, $\phi(t) = \pm 2\pi t/T$. In the counterclockwise example the solution matches the adiabatic prediction and the corresponding state flips, but in the clockwise example we observe a nonadiabatic transition, for which, apart from an overall amplification, the system returns to the original state. This chiral behavior, first presented in Ref. [25], illustrates one of the key differences between the dynamics in Hermitian and non-Hermitian systems. In the latter, the eigenvalues are complex, which causes gain or loss in c_- and c_+. An infinitesimally small nonadiabatic coupling can therefore be exponentially amplified, causing the gain eigenvector to dominate. This mechanism intuitively explains why the adiabatic theorem does not in general hold for non-Hermitian systems.

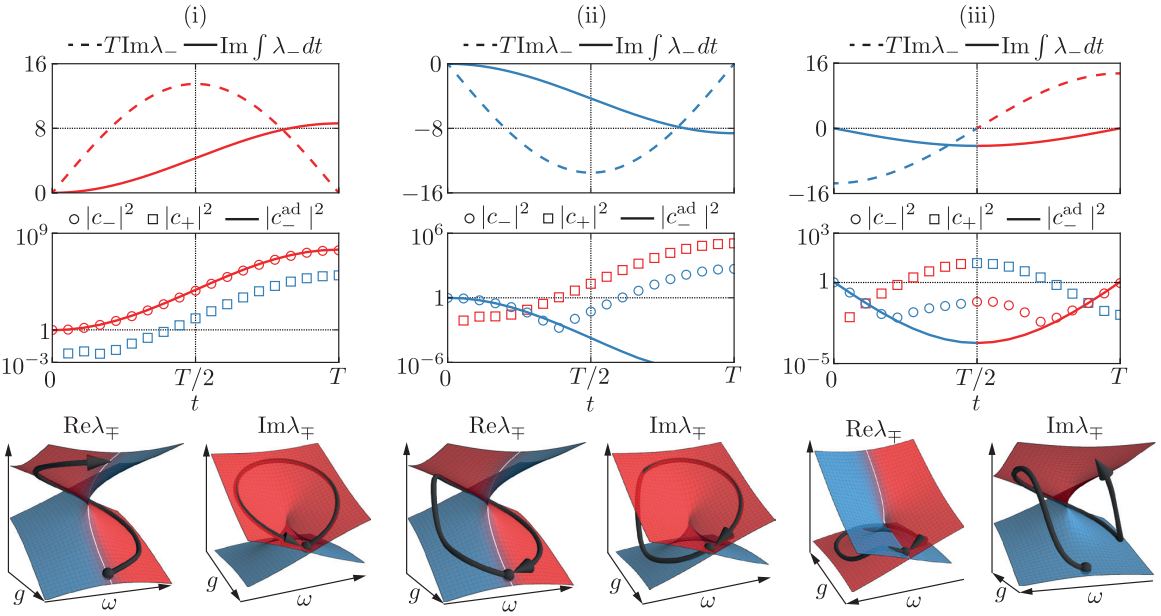

FIG. 2. (Color online) Plots of typical numerical solutions of Eq. (3) for the path defined in Fig. 1(b) with initial eigenvector populations $c_-(0) = 1$ and $c_+(0) = 0$. For the function ϕ we choose $\phi(t) = \pm 2\pi t/T$ in examples (i) and (ii) and we choose $\phi(t) = -2\pi t/T + \pi$ in example (iii). In all cases we set $r = 0.1$, $\gamma = 1$, and $T = 45$, for which $T|\lambda_- - \lambda_+| \gg 1$. The top row shows the dynamical gain parameter $T\,\mathrm{Im}\lambda_-(t)$ and the total integrated gain $\int_0^t \mathrm{Im}\lambda_-(t')dt'$. Note that the dynamical gain is the gain of the adiabatic prediction but not necessarily the actual gain of the numerical solution. The middle row shows the eigenvector populations $|c_\mp(t)|^2$ along with the adiabatic prediction $|c_-^{\mathrm{ad}}(t)|^2$. We do not plot $|c_+^{\mathrm{ad}}(t)|^2$ because adiabatic principles imply $|c_+^{\mathrm{ad}}(t)|^2 \ll |c_-^{\mathrm{ad}}(t)|^2$. The bottom row shows a projection of the numerical solution onto the real and imaginary parts of the eigenspectrum, specifically $[|c_-(t)|^2\lambda_-(t) - |c_+(t)|^2\lambda_+(t)]/[|c_-(t)|^2 + |c_+(t)|^2]$. The use of red and blue is to provide an indication of which population, or surface, corresponds to a gain and loss eigenvector, respectively.

Example (iii) shows the result for a more interesting path $\phi(t) = -2\pi t/T + \pi$ where gain-loss behavior swaps halfway through and the total integrated dynamical gain vanishes $\int_0^T \mathrm{Im}\lambda(t)dt = 0$. Surprisingly, the final state matches the adiabatic prediction $|c_-(T)|^2 \simeq |c_-(0)|^2$ even though during the interim the solution is highly nonadiabatic. This observation cannot be explained by the intuitive argument above because c_- is nontrivially slaved to c_+ past the time $t = T/2$ when we would expect c_- to increase exponentially. Thus, considering dynamical gain alone is insufficient to accurately predict behavior for quasiadiabatic dynamics near EPs.

These basic examples illustrate that the dynamics of non-Hermitian systems involves three characteristic effects: (i) the swapping of eigenvectors due to a 4π periodicity about an EP, which follows from the topology of the complex eigenvalue spectrum, (ii) the appearance of enhanced nonadiabatic transitions due to the presence of gain or loss, and (iii) periods of adiabatic evolution that persist significantly beyond the time of stability loss. While (i) is readily incorporated by the eigenvector decomposition (6), we will now develop a general approach to describe the nontrivial interplay between (ii) and (iii).

III. DYNAMICAL ANALYSIS

A. Relative nonadiabatic transition amplitudes

In order to develop a general dynamical description we consider the evolution operator $\mathcal{U}(t)$ defined by $\vec{x}(t) = \mathcal{U}(t)\vec{x}(0)$, which contains the full dynamics independent of the initial condition. In the eigenbasis Eq. (5), $\mathcal{U}(t)$ is the solution of

$$\dot{\mathcal{U}} = -i\begin{pmatrix} -\lambda(t) & -f(t) \\ f(t) & \lambda(t) \end{pmatrix}\mathcal{U}, \quad \mathcal{U} = \begin{pmatrix} \mathcal{U}_{-,-} & \mathcal{U}_{-,+} \\ \mathcal{U}_{+,-} & \mathcal{U}_{+,+} \end{pmatrix}, \tag{7}$$

with initial condition $\mathcal{U}(0) = \mathbb{1}$, where

$$f(t) = \frac{g(t)[\dot{\omega}(t) + i\dot{\gamma}(t)/2] - [\omega(t) + i\gamma(t)/2]\dot{g}(t)}{2i\lambda^2(t)} \tag{8}$$

is the nonadiabatic coupling. Adiabaticity usually requires that the nonadiabatic coupling be much smaller than the distance between eigenvectors $\varepsilon(t) := |f(t)/2\lambda(t)| \ll 1$. Since $\varepsilon(t) \propto T^{-1}$ this condition is always satisfied for an appropriate T. Setting $f(t) = 0$ in Eq. (7), which would imply $\varepsilon(t) = 0$, would yield the diagonal adiabatic prediction

$$\mathcal{U}^{\mathrm{ad}}(t) = \begin{pmatrix} \exp\left(i\int_0^t \lambda(t')dt'\right) & 0 \\ 0 & \exp\left(-i\int_0^t \lambda(t')dt'\right) \end{pmatrix}. \tag{9}$$

However, as is evident in Fig. 2, even for arbitrarily small yet nonvanishing $\varepsilon(t)$ the actual solution is significantly nondiagonal. This indicates that the system is singularly perturbed by the nonadiabatic coupling and $\mathcal{U}(t)$ cannot be obtained as a perturbative correction to $\mathcal{U}^{\mathrm{ad}}(t)$. We shall henceforth call $\varepsilon(t) \ll 1$ the quasiadiabatic condition (see Appendix A for more details).

In order to describe the nonadiabatic character of $\mathcal{U}(t)$ for quasiadiabatic dynamics we focus on the relative nonadiabatic transition amplitudes [25]

$$R_-(t) := \frac{\mathcal{U}_{+,-}(t)}{\mathcal{U}_{-,-}(t)}, \quad R_+(t) := \frac{\mathcal{U}_{-,+}(t)}{\mathcal{U}_{+,+}(t)}. \tag{10}$$

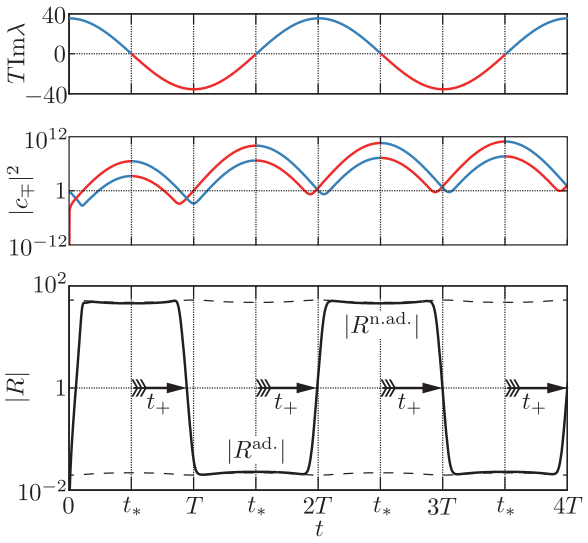

FIG. 3. (Color online) Plot of $\mathrm{Im}\lambda(t)$ (top panel), $|c_{\mp}|^2$ (middle panel), and a typical solution for $R \equiv R_-$ (bottom panel) for the path defined in Fig. 1(b) with $\phi(t) = -2\pi t/T + \pi$. Note that $\mathrm{Im}\lambda(t) = -\mathrm{Im}\lambda_-(t)$, which is plotted in Fig. 2. We have chosen $r = 0.1$, $\gamma = 1$, and $T = 120$, for which $\varepsilon(t) \simeq 2.5\%$. The solid curve is the numerical solution. The arrows denote delay times. The lower and upper dashed grid lines denote $|R^{\mathrm{ad}}(t)|$ and $|R^{\mathrm{nad}}(t)|$, respectively.

These describe the amount of nonadiabaticity in the solution. For example, $R_-(t)$ is a measure of the magnitude of the net nonadiabatic transition from $\vec{r}_-(t)$ to $\vec{r}_+(t)$, i.e., $R_-(t) = c_+(t)/c_-(t)$ given $c_-(0) = 1$ and $c_+(0) = 0$. If $R_{\mp}(t) \ll 1$ then we may say that $c_{\mp}$ is behaving adiabatically, while $R_{\mp}(t) \gg 1$ indicates that a nonadiabatic transition has occurred. From Eqs. (7) and (10) it follows that $R_{\mp}(t)$ considered as a dynamical variable is the solution to the Riccati equation [31,46]

$$\dot{R}_{\mp} = \mp 2i\lambda(t)R_{\mp} \mp if(t)(1 + R_{\mp}^2), \tag{11}$$

with initial condition $R_{\mp}(0) = 0$. Dynamical phenomena associated with quasiadiabatically encircling EPs can thus be understood from the solutions of this equation in the limit $\varepsilon(t) \ll 1$. Note that the equations of motion for R_- and R_+ are related via $R_- \leftrightarrow 1/R_+$. In the following, we therefore consider only $R := R_-$ without loss of generality. We remark that, assuming transients are damped, the relation $R_- \leftrightarrow R_+$ has the immediate consequence that $\lim_{t\to\infty} R_-(t)R_+(t) = 1$, which agrees with Ref. [25] and prohibits simultaneous adiabatic behavior in both c_- and c_+ over long times.

B. Fixed points and stability loss delay

The lower panel of Fig. 3 shows a generic solution for R during multiple quasiadiabatic encirclements of an EP (see the caption for details). It resembles a square wave, i.e., we see fast switching between two quasistationary values. This behavior can be understood from a separation of time scales in Eq. (11). For short times the slowly varying parameters $\lambda(t) \simeq \lambda$ and $f(t) \simeq f$ can be considered constant and

$$\dot{R} \simeq -2i\lambda R - if(1 + R^2). \tag{12}$$

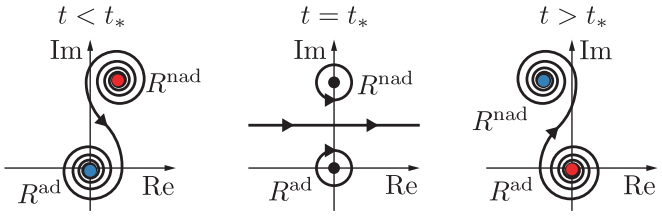

FIG. 4. (Color online) Cartoons of the global phase portraits of the equation of motion for R near t_*. Arrows denote the direction of time evolution along an integral curve. The fixed point near the origin corresponds to $R^{\mathrm{ad}}(t)$ and the fixed point far from the origin corresponds to $R^{\mathrm{nad}}(t)$.

On a fast time scale set by $|\mathrm{Im}\lambda|^{-1}$ the solution therefore approaches one of two fixed points

$$\begin{aligned} R^{\mathrm{ad}} &= -\frac{\lambda}{f}\left(1 - \frac{\sqrt{\lambda^2 - f^2}}{\lambda}\right) \simeq -\frac{f}{2\lambda}, \\ R^{\mathrm{nad}} &= -\frac{\lambda}{f}\left(1 + \frac{\sqrt{\lambda^2 - f^2}}{\lambda}\right) \simeq -\frac{2\lambda}{f}. \end{aligned} \tag{13}$$

The first fixed point $R^{\mathrm{ad}}(t) \propto \varepsilon(t) \ll 1$ indicates adiabatic behavior (c_- dominates) and, by inspecting Eq. (11), is stable for $\mathrm{Im}\lambda(t) < 0$. The second fixed point $R^{\mathrm{nad}}(t) \propto \varepsilon^{-1}(t) \gg 1$ indicates a nonadiabatic transition has occurred (c_+ dominates) and is stable for $\mathrm{Im}\lambda(t) > 0$. These two fixed points are plotted in Fig. 3. Evidently, the periods of quasistationarity there exhibited correspond to following one of these two fixed points.

On a slow time scale set by T the parameters $\lambda(t)$ and $f(t)$ may change considerably and at certain critical times the stability of the two fixed points swaps. For example, $R^{\mathrm{ad}}(t)$ becomes unstable and $R^{\mathrm{nad}}(t)$ stable when the sign of $\mathrm{Im}\lambda(t)$ becomes positive. Let us denote the critical times by t_*, which are marked in Fig. 3. Naively, one might expect an immediate rapid transition between the neighborhoods of $R^{\mathrm{ad}}(t)$ and $R^{\mathrm{nad}}(t)$ upon passing a critical time t_*, but, as is evident in Fig. 3, this is not the case. Instead, we see that the solution follows, e.g., $R^{\mathrm{ad}}(t)$, while it is unstable for a significant amount of time; the loss in stability is delayed. Intuition for this behavior is obtained from the phase portraits of Eq. (11), shown in Fig. 4. The local phase portrait about $R^{\mathrm{ad}}(t)$ goes from a spiral towards $R^{\mathrm{ad}}(t)$ for $t < t_*$ to a spiral away from $R^{\mathrm{ad}}(t)$ for $t > t_*$, passing through a degenerate bifurcation at $t = t_*$ when $R^{\mathrm{ad}}(t)$ is a center and is neither stable nor unstable. We therefore expect some persistence in the following of $R^{\mathrm{ad}}(t)$ because near t_* it is only weakly stable or unstable.

To illustrate the existence of a significant delay between the critical time t_* and the actual time of a nonadiabatic transition t_+ we consider the specific path defined in Fig. 1(b) with $\phi(t) = -2\pi t/T + \pi$ and $r \ll \gamma$. This is a good model for the numerical solution shown in Fig. 3. Then $\lambda(t) \simeq i\sqrt{r\gamma}e^{-i\pi t/T}$, $f(t) \simeq i\pi/2\,T$, and $\varepsilon(t) \simeq \varepsilon = \pi/4\sqrt{r\gamma}\,T$. Let us focus on the loss of stability of $R^{\mathrm{ad}}(t)$ at $t_* = 3T/2$. Assuming that the system is near $R^{\mathrm{ad}}(t)$, we can neglect the nonlinear term in

Eq. (11):

$$\frac{\dot{R}}{2\sqrt{r\gamma}} \simeq e^{-i\pi t/T} R + \varepsilon. \tag{14}$$

The particular integral of this equation is found to be

$$R(t) = -\frac{i}{2} E_1\left(\frac{i}{2\varepsilon} e^{-i\pi t/T}\right) e^{i\exp(-i\pi t/T)/2\varepsilon}, \tag{15}$$

where E_1 is the exponential integral. Since $\varepsilon \ll 1$ we may use the asymptotic expansion for E_1 (see, e.g., 5.1.7 and 5.1.51 in Ref. [47]) to obtain

$$R(t) \simeq -\varepsilon e^{i\pi t/T} - 2i\varepsilon^2 e^{2i\pi t/T} + \cdots - \frac{\pi}{2}\,\mathrm{sgn}\left[\cos\left(\frac{\pi t}{T}\right)\right] e^{i\cos(\pi t/T)/2\varepsilon} e^{\sin(\pi t/T)/2\varepsilon}. \tag{16}$$

The first two terms (first line on the right-hand side) correspond to following $R^{\mathrm{ad}}(t)$ with higher-order corrections. The third term (second line) is negligible for $t - t_* < T/2$ (recall $t_* = 3T/2$ here), but it diverges exponentially for $t - t_* > T/2$, thereby indicating a nonadiabatic transition. Thus, under the ideal conditions assumed here and given that the solution has approached $R^{\mathrm{ad}}(t)$ by $t = t_*$, the delay in the loss of stability is $t_+ - t_* = T/2$.

With this analysis we are already in a position to understand better the three examples studied in Fig. 2. In example (i) $R^{\mathrm{ad}}(t)$ is stable for the entire loop around the EP and therefore the solution follows the adiabatic prediction $|c_+(t)/c_-(t)| \simeq |R^{\mathrm{ad}}(t)|$. In contrast, in (ii) $R^{\mathrm{ad}}(t)$ is always unstable and a nonadiabatic transition occurs. In (iii) the solution first switches from $R^{\mathrm{ad}}(t)$ to $R^{\mathrm{nad}}(t)$, but then back again with a delay $t_+ \lesssim T/2$ after $R^{\mathrm{ad}}(t)$ becomes stable at $t = T/2$. Note that the delay times exhibited in the first encircling period as shown in Figs. 2 and 3 differ from the value $t_+ = T/2$ estimated above. This is due to a high sensitivity to the initial condition $R(0) = 0$, which is not exponentially close to $R^{\mathrm{ad}}(0)$, and therefore effects a transient term of the form $Ae^{i\exp(-i\pi t/T)/2\varepsilon}$. After about one encircling period the system approaches the unique long-time relaxation oscillation, which is a universal signature of quasiadiabatically encircling EPs.

We finish this section with a remark on the relation between the above results and the Stokes phenomenon of asymptotics, i.e., the switching on of exponentially suppressed terms in asymptotic expansions [32]. In Refs. [26,31] an exact solution for the example considered in this section is presented (using $r \ll \gamma$ but not neglecting the nonlinearity), which we review in Appendix B. In this exact solution one sees that the sharp (but continuous) transition, which in Eq. (16) is represented by the signum function, is precisely the Stokes phenomenon of asymptotics, leading here to a breakdown of the adiabatic theorem. In our current approach, which we elaborate further in the next section, this discontinuity is connected to the problem of stability loss delay. The connection between the Stokes phenomenon of asymptotics and stability loss delay might be worth exploring further. However, here we will leave such considerations aside and proceed with a pragmatic generalization of these initial results to arbitrary paths in parameter space.

C. Generalized quasiadiabatic solution

In Sec. III B we were able to understand the generic solution exhibited in Fig. 3 from a separation of time scales, which resulted in a delay in the loss of stability of the instantaneous fixed points. In fact, slow-fast systems with dynamical bifurcations are a subject of current mathematical interest. The reader is referred to Ref. [33] for a concise description. The reason that the critical times do not coincide with the observed times when an instantaneous fixed point loses stability is because our slow-fast system is singularly perturbed; the slow system is described by an algebraic equation and the fast system by a differential equation. One must therefore resort to nonstandard analysis. A principal result of the nonstandard analysis of slow-fast systems is the existence of stability loss delay about certain dynamical bifurcations [34,35,48], which we observed explicitly in Sec. III B. In the following we build upon this to construct a generalized quasiadiabatic solution, which, additionally, affords an estimation of delay times.

We are interested in solutions that for times near critical times t_* are in the vicinity of a fixed point. We therefore begin by looking at the zero crossings of $\mathrm{Im}\lambda(t)$, which determine t_*. For some window $[t_-,t_+]$ about each t_*, i.e., $t_- < t_* < t_+$, we seek a solution $R_{t_*}(t)$ that follows $R^{\mathrm{ad}}(t)$ or $R^{\mathrm{nad}}(t)$. Since transitions between $R^{\mathrm{ad}}(t)$ and $R^{\mathrm{nad}}(t)$ are very quick, by making a piecewise addition of segments that follow one or the other fixed point we arrive at the approximation for the complete solution thus

$$R(t) \simeq \sum_{t_*} [\Theta(t - t_-) - \Theta(t - t_+)] R_{t_*}(t), \tag{17}$$

where Θ is the Heaviside step function.

Let us now consider a single segment and omit the subscript t_* for brevity. We may focus on the case that $R(t)$ follows $R^{\mathrm{ad}}(t)$ without loss of generality because $R^{\mathrm{nad}}(t) = 1/R^{\mathrm{ad}}(t)$ and Eq. (11) is antisymmetric under the transformation $R \mapsto 1/R$. Since we assume $R(t)$ to be in the vicinity of $R^{\mathrm{ad}}(t)$ for $t \in [t_-,t_+]$ we study the linearized equation of motion about $R^{\mathrm{ad}}(t)$:

$$\dot{R} = -2i\lambda(t)R - if(t). \tag{18}$$

The general solution from time $t = t_0$ of this equation is

$$R(t) = R(t_0)e^{\Psi(t)-\Psi(t_0)} - i\int_{t_0}^{t} dt' f(t') e^{\Psi(t)-\Psi(t')}, \tag{19}$$

where $R(t_0)$ is the initial condition and

$$\Psi(t) = -2i\int_{t_*}^{t} \lambda(t')dt'. \tag{20}$$

Note that, to first order about t_* we have $\lambda(t) = \lambda(t_*) + \dot{\lambda}(t_*)(t - t_*) + O((t - t_*)^2)$. Since $\mathrm{Im}\lambda(t_*) = 0$ and $\mathrm{Im}\dot{\lambda}(t_*) > 0$ then $\mathrm{Re}\Psi(t) = \mathrm{Im}\dot{\lambda}(t_*)(t - t_*)^2 + O((t - t_*)^3)$ is convex. We refer to this property of Ψ below. Integrating the integral in Eq. (19) by parts N times yields

$$R(t) = [R(t_0) - \mathcal{R}^{\mathrm{ad}}(t_0)]e^{\Psi(t)-\Psi(t_0)} + \mathcal{R}^{\mathrm{ad}}(t) + \Delta(t)e^{\Psi(t)}. \tag{21}$$

Here we have introduced

$$\mathcal{R}^{\rm ad}(t) = \sum_{n=0}^{N-1} \left(\frac{-1}{2i\lambda(t)} \frac{d}{dt} \right)^n R^{\rm ad}(t), \tag{22}$$

which encapsulates the following of $R^{\rm ad}(t)$: The $n = 0$ term in $\mathcal{R}^{\rm ad}(t)$ is simply $R^{\rm ad}(t)$ and the higher-order terms are corrections due to finite variations in $\lambda(t)$ and $f(t)$. However, since each term in the sum contains a derivative and therefore scales with $n!$, there is an optimal truncation $N = N_{\rm op}$ beyond which the sum diverges. The precise value of $N_{\rm op}$ is problem specific, but for most purposes including only the first few terms in the sum (22) is sufficient.

The final term in Eq. (21), $\Delta(t)e^{\Psi(t)}$, is the remaining part of the solution that is not included in the sum (22). It therefore describes the nontrivial part of the dynamics that inevitably causes a departure from $R^{\rm ad}(t)$. Since $\Delta(t)e^{\Psi(t)}$ is the remainder of an optimally truncated sum it is negligible whenever the solution follows $R^{\rm ad}(t)$. On the other hand, for times $t \approx t_+$ when $\Delta(t)e^{\Psi(t)}$ starts to dominate, $\mathcal{R}^{\rm ad}(t)$ is negligible and we may approximate

$$\Delta(t)e^{\Psi(t)} \simeq -ie^{\Psi(t)} \int_{t_0}^{t} dt' f(t')e^{-\Psi(t')}. \tag{23}$$

Since $\mathrm{Re}\Psi$ is convex and since $\Psi(t) \propto \varepsilon^{-1}(t)$, the integrand in Eq. (23) is non-negligible only for times $t' \approx t_*$ and the value of Δ becomes quite independent of $t > t_*$ and $t_0 < t_*$. Therefore, under quite general conditions, we can approximate $\Delta(t)e^{\Psi(t)} \simeq \Theta(t - t^*)\Delta e^{\Psi(t)}$, where Θ is the Heaviside step function and

$$\Delta = -i \int_{t_-}^{t_+} dt f(t)e^{-\Psi(t)}. \tag{24}$$

The precise values of t_- and t_+ are of little importance in the evaluation of this integral, only that they are far enough from t_* that the integrand is negligible at them. We thus arrive at

$$R(t) \simeq \mathcal{R}^{\rm ad}(t) + [A + \Theta(t - t_*)\Delta]e^{\Psi(t)}, \tag{25}$$

where $A = [R(t_0) - \mathcal{R}^{\rm ad}(t_0)]e^{-\Psi(t_0)}$ depends on the initial condition.

From Eq. (25) and the analogous expression for a segment that follows $R^{\rm nad}(t)$, we construct our piecewise addition of segments by determining the exit time t_+ of a segment from the condition $|R(t_+)| = 1$, i.e., when the solution is halfway between $R^{\rm ad}(t)$ and $R^{\rm nad}(t)$, and then using this as the entry time t_- for the next segment. Two effects may cause this transition. First, if the solution does not have enough time to approach, e.g., $R^{\rm ad}(t)$ sufficiently closely by the critical time, then the finite difference $|R(t_*) - R^{\rm ad}(t_*)|$ will be exponentially amplified after $t = t_*$. This mechanism is responsible, e.g., for the initial transitions one observes in a single encircling of an EP, where the system is initialized to $R(0) = 0 \not\approx R^{\rm ad}(t)$. Second, however, we see that even for $A = 0$ a destabilization occurs due to a dynamical mechanism represented by $\Delta \neq 0$, which yields the time of stability loss t_+ via

$$|\Delta e^{\Psi(t_+)}| = 1. \tag{26}$$

The time t_+ determined in this way is independent of transients and therefore characterizes the longest time the solution can remain stable after t_*. In the quasiadiabatic limit $\varepsilon(t) \to 0$ this is independent not only of transients but also of adiabaticity and is in fact the so-called maximal delay time t_+^* (see Appendix A 5 for more details).

D. Analytic examples

Here we consider three examples analytically in order to illustrate our generalized quasiadiabatic solution: a circular $\lambda(t)$ as in Sec. III B, a linear $\lambda(t)$ corresponding to the lowest-order Taylor expansion, and an elliptical $\lambda(t)$ corresponding to the lowest-order Fourier expansion. The first example serves to verify that our generalized quasiadiabatic solution recovers the more specific analytic results in Sec. III B. The second and third examples serve to illustrate the sensitivity of Δ and therefore t_+ in Eq. (26) to the global path—stability loss delay is a global phenomenon. Note that a circular, elliptical, or linear $\lambda(t)$ does not precisely correspond to a circular, elliptical, or linear path in parameter space unless we are in, say, the limit $r \ll 1$. We study particular paths in parameter space numerically in Sec. III E.

(i) Circular $\lambda(t)$. From Sec. III B,

$$\lambda(t) = i\sqrt{r\gamma}e^{-i\pi t/T}, \tag{27}$$

$$f(t) = \frac{i\pi}{2T}. \tag{28}$$

The adiabatic fixed point with corrections is

$$\mathcal{R}^{\rm ad}(t) = -\varepsilon e^{i\pi t/T} \sum_{n=0}^{N-1} n!(2i\varepsilon e^{i\pi t/T})^n, \tag{29}$$

where $\varepsilon = \pi/4\sqrt{r\gamma}T$ and the optimal truncation is $N_{\rm op} \sim (2\varepsilon)^{-1}$. Furthermore, about $t_* = 3T/2$,

$$\Psi(t) = \frac{1}{2\varepsilon}(ie^{-i\pi t/T} + 1), \tag{30}$$

$$\Delta = -\pi e^{-1/2\varepsilon}. \tag{31}$$

Putting these expressions together in Eq. (25) recovers Eq. (16) and solving for t_+ in Eq. (26) yields the delay time

$$t_+ - t_* = \frac{T}{\pi} \arccos(2\varepsilon \log \pi), \tag{32}$$

which in the limit $\varepsilon \to 0$ becomes $t_+ - t_* = T/2$, in agreement with Sec. III B.

(ii) Linear $\lambda(t)$. Let us now consider another important scenario, where the line of instability is crossed in a linear sweep,

$$\lambda(t) = \lambda_{\rm Re} + i\dot{\lambda}_{\rm Im}t, \tag{33}$$

$$f(t) \simeq f(t_*) = \text{const}, \tag{34}$$

where $\dot{\lambda}_{\rm Im} > 0$. In this case we have $\Psi(t) = -2i\lambda_{\rm Re}t + \dot{\lambda}_{\rm Im}t^2$ about $t_* = 0$ and the discontinuity is

$$\Delta = -if(t_*)\sqrt{\frac{\pi}{\dot{\lambda}_{\rm Im}}}e^{-\lambda_{\rm Re}^2/\dot{\lambda}_{\rm Im}}. \tag{35}$$

From these expressions we deduce the delay time

$$t_+ - t_* = \frac{\lambda_{\mathrm{Re}}}{\dot{\lambda}_{\mathrm{Im}}}\sqrt{1+\frac{\dot{\lambda}_{\mathrm{Im}}}{\lambda_{\mathrm{Re}}^2}\log\left(\sqrt{\frac{\dot{\lambda}_{\mathrm{Im}}}{\pi}}\frac{1}{|f(t_*)|}\right)}, \tag{36}$$

which in the quasiadiabatic limit becomes $t_+ - t_* = \lambda_{\mathrm{Re}}/\dot{\lambda}_{\mathrm{Im}}$. One might naively hypothesize that Eq. (35) describes more general paths by using $\lambda_{\mathrm{Re}} = \mathrm{Re}\lambda(t_*)$ and $\lambda_{\mathrm{Im}} = \mathrm{Im}\dot{\lambda}(t_*)$. However, a comparison with the circular path above already shows that this would only give rather poor quantitative results. Equation (36) may still serve as a first estimate of the expected delay times in general scenarios.

(iii) Elliptical $\lambda(t)$. As an interpolation between the two cases above we consider the lowest-order Fourier expansion of $\lambda(t)$ about $t = t_*$:

$$\lambda(t) = \lambda_{\mathrm{Re}}\cos(\pi t/T) + i\frac{T\dot{\lambda}_{\mathrm{Im}}}{\pi}\sin(\pi t/T), \tag{37}$$

$$f(t) \simeq f(t_*) = \text{const.} \tag{38}$$

With $\lambda_{\mathrm{Re}} = T\dot{\lambda}_{\mathrm{Im}}/\pi = \sqrt{r\gamma}$ one recovers the circular $\lambda(t)$ and for $T \to \infty$ but keeping $\dot{\lambda}_{\mathrm{Im}}$ fixed one recovers the linear sweep of $\lambda(t)$. For this example the discontinuity is

$$\Delta = -2iTf(t_*)e^{-2T^2\dot{\lambda}_{\mathrm{Im}}/\pi^2} I_0\left(\frac{2T}{\pi}\sqrt{\frac{T^2\dot{\lambda}_{\mathrm{Im}}^2}{\pi^2} - \lambda_{\mathrm{Re}}^2}\right), \tag{39}$$

where I_0 is the first-order modified Bessel function of the first kind. By taking the appropriate limits—$I_0(x) \sim 1$ for $x \ll 1$ and $x \in \mathbb{R}^+$ (see, e.g., 9.6.7 in Ref. [47]) for the circular $\lambda(t)$ and $I_0(x) \sim e^x/\sqrt{2\pi x}$ for $x \gg 1$ and $x \in \mathbb{R}^+$ (see, e.g., 9.6.30 and 9.7.1 in Ref. [47]) for the linear $\lambda(t)$—one recovers either Eq. (31) or (35). Therefore, Eq. (39) interpolates between the two limiting cases above and can be used to accurately calculate delay times for situations where the encircling path lies somewhere in between.

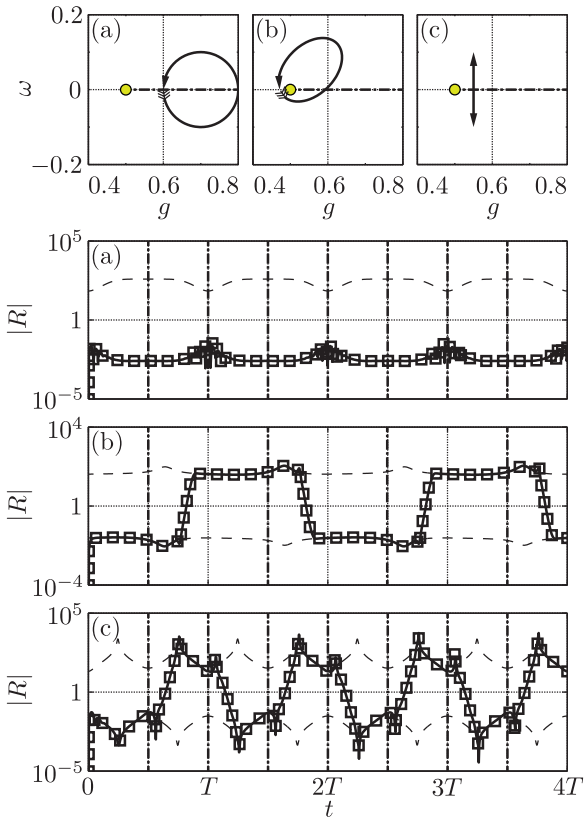

FIG. 5. (Color online) Plots of $|R(t)|$ (three bottom panels) for three different paths (top row). In every plot of $|R(t)|$ the solid line is our generalized quasiadiabatic solution, the open squares denote the numerical solution, the dashed lines denote $\mathcal{R}^{\mathrm{ad}}(t)$ and $\mathcal{R}^{\mathrm{nad}}(t)$, and the dot-dashed lines denote critical times t_*. For the plots of the path, the yellow-filled circle marks the position of the EP and the dot-dashed line is the critical line where $\mathrm{Im}\lambda = 0$. The parameter settings chosen are (a) $r = 0.1$, $T = 200$, and $g_{\mathrm{os}} = 0.2$; (b) $r = 0.1$, $T = 200$, $e = 0.75$, and $\theta_{\mathrm{aa}} = \pi/4$; and (c) $L = 0.2$, $T = 200$, and $g_{\mathrm{os}} = 0.05$ (see the main text for details on the parametrization).

E. Numerical examples

Let us now demonstrate the validity of our approach numerically for more general examples depicted in Fig. 5: (a) a displaced circular path $\omega(t) = r\sin\phi(t)$ and $g(t) = \gamma/2 + r\cos\phi(t) + g_{\mathrm{os}}$, where $\phi(t) = 2\pi t/T$ and g_{os} is a variable offset in the coupling; (b) a tilted elliptical path $\omega(t) = r(t)\sin\phi(t)$ and $g(t) = \gamma/2 + r(t)\cos\phi(t)$, where $\phi(t) = 2\pi t/T$, $r(t) = r_0(1-e^2)/\{1 + e\cos[\phi(t) + \theta_{\mathrm{aa}}]\}$, e is the ellipticity, and θ_{aa} is the angle of the apoapsis; and (c) oscillations along a straight path that crosses the critical line $\omega(t) = -L\sin\phi(t)$ and $g(t) = \gamma/2 + g_{\mathrm{os}}$, where $\phi(t) = 2\pi t/T$. For these examples the numerically simulated solution $R(t)$ is plotted in Fig. 5 and compared with the generalized quasiadiabatic solution presented in Sec. III C, with Δ being evaluated numerically. We see that in all cases the numerical and analytic results match up perfectly.

Let us first consider path (a). For this path there are two dynamical bifurcations in every period, as indicated, but the departure time as determined by Eq. (26) is infinite. Therefore, the solution never has enough time to be significantly repelled from $R^{\mathrm{ad}}(t)$ before $R^{\mathrm{ad}}(t)$ becomes stable once again. As a result, the system never leaves the neighborhood of $R^{\mathrm{ad}}(t)$, i.e., the solution is adiabatic. In some sense, the increased frequency of dynamical bifurcations and the long departure time has stabilized the adiabatic prediction. In path (b) the opposite is the case. Here the solution undergoes a nonadiabatic transition every period. The solution looks quite similar to that shown in Fig. 5(a), except that the nonadiabatic transitions occur earlier. One finds in this case that the delay time is roughly $0.32T$, slightly less than $T/2$. Finally, in path (c) we have chosen again a path with two dynamical bifurcations per period, but in this case the departure time is roughly $0.15T$, significantly less than $T/2$. Accordingly, we observe two nonadiabatic transitions per period.

The last case can in fact be made to resemble either of the former two cases by tuning g_{os}, i.e., by changing the value of $\lambda_{\mathrm{Re}}(t_*)$. In Fig. 6 we have plotted the departure time as a function of g_{os}. For $g_{\mathrm{os}} < 0.05$ the quasiadiabatic condition breaks down. For $0.05 < g_{\mathrm{os}} \lesssim 0.12$, i.e., close to the EP, the solution resembles Fig. 5(c) and we observe two nonadiabatic transitions in every period. Around $g_{\mathrm{os}} = 0.12$ the departure

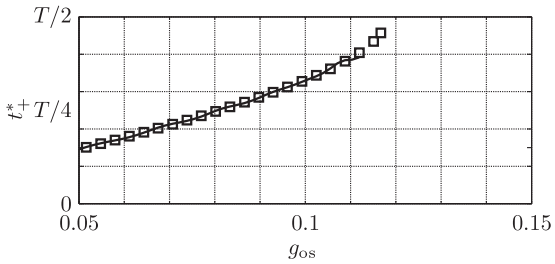

FIG. 6. Plot of the departure time t_+ for path (c) in Fig. 5 with the same parametrization, except for g_{os}, which we vary. The solid line is t_+ as determined by Eq. (26) and the open squares denote the numerically observed departure time as determined via $|R(t)| = 1$. Good agreement is exhibited between the analytic t_+ and the numerical t_+. A particularly interesting feature is that t_+ becomes infinite for $g_{os} \gtrsim 0.12$. For large g_{os} one then expects the system to remain adiabatic for all times, as observed in Fig. 5(a).

time becomes infinite, which implies that for $g_{os} \gtrsim 0.12$ the dynamics becomes fully adiabatic and resembles Fig. 5(a).

IV. NOISE

Finally, it is important to address the influence of noise, which will be present in any experimental implementation. To do so we simulated the dynamics of $c_\mp$ in the presence of δ-correlated Gaussian noise $\xi(t)$ with variance $\langle \xi(t)\xi(t')\rangle = \gamma N \delta(t - t')$. The gray shaded area in Fig. 7 indicates the resulting distribution of stochastic trajectories of $R(t)$ for $N = 1/10$. This resembles the case where the initial resonator amplitude is a factor of 10 above the thermal noise floor. For the first encircling period the fixed point $R^{\text{nad}}(t)$ is still robust, but the delay time t_+ is significantly reduced. This again demonstrates the extreme sensitivity of Eq. (11) upon initial conditions. However, the dynamics of R is self-correcting and after the first encircling period it settles into robust periodic dynamics much resembling the case without noise. This surprising observation can be understood as follows. Initially, noise causes R to lose stability early; however, this means that the total population of the system is increased and therefore the effect of the constant noise background is reduced.

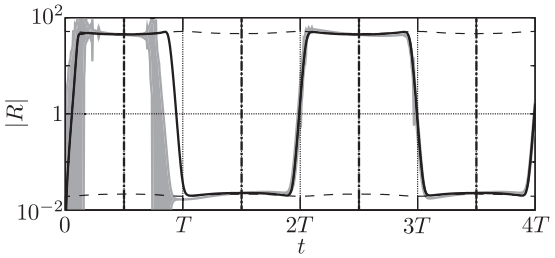

FIG. 7. Here we reproduce the solution from the bottom panel of Fig. 3 with our analytic prediction (solid line) with a stochastic spread (shaded area). Specifically, the shaded area is one standard deviation about the mean of R obtained from 10 000 stochastic numerical integrations of c_- and c_+ (see Sec. IV for more details).

V. CONCLUSION

In summary, we have analyzed the quasiadiabatic evolution of non-Hermitian systems near an EP. Our study shows that various dynamical phenomena associated with this process can be predicted from the analysis of the nonadiabatic transition amplitudes $R_-(t)$ and $R_+(t)$. In particular, we identified a characteristic switching pattern and stability loss delay. Our analytic predictions for the delay times and the observed robustness with respect to noise are relevant for experimental investigations of these effects and provide the basis for analyzing similar phenomena in more complex systems.

ACKNOWLEDGMENTS

The authors thank M. V. Berry, E.-M. Graefe, M. Koller, D. O. Krimer, A. Mailybaev, A. Neishtadt, and R. Uzdin for useful input. This work was supported by the European FP7/ITC Project SIQS (No. 600645), Project OPSOQI (No. 316607) of the WWTF, the Austrian Science Fund (FWF) through SFB FOQUS F40, SFB NextLite F49-10, Project GePartWave No. I 1142-N27, the START Grant No. Y 591-N16 and the CoQuS doctoral programme, DK CoQuS W 1210.

APPENDIX A: NONSTANDARD ANALYSIS OF RELATIVE NONADIABATIC TRANSITION AMPLITUDES

In this Appendix we briefly summarize the motivation for the nonstandard analysis of quasiadiabatic non-Hermitian systems [23,44,45] and its application to relative nonadiabatic transition amplitudes [33,48–51]. In order to facilitate a simple but rigorous mathematical treatment we augment the notation of the paper by introducing a dimensionless time

$$s := \frac{t}{T}, \tag{A1}$$

where T^{-1} is considered small, and rewrite the governing equation of motion

$$\dot{\mathcal{U}} = -i\mathbf{M}(s)\mathcal{U}, \tag{A2}$$

with $\mathcal{U}(0) = 1$ and where $\mathcal{U}$ is the evolution operator and the dot denotes the derivative with respect to time t as usual.

1. Quasiadiabaticity

We assume $\mathbf{M}(s)$ to be diagonalizable with eigenvalues $\lambda_i(s)$ for all s. Since $\mathbf{M}(s)$ is non-Hermitian it does not in general have an orthonormal eigenbasis in the sense of Dirac but rather a biorthogonal eigenbasis: a set of right eigenvectors $\vec{r}_i(s)$ defined via $\mathbf{M}(s)\vec{r}_i(s) = \lambda_i(s)\vec{r}_i(s)$ and a set of left eigenvectors $\vec{l}_i^{\,T}(s)$ defined via $\vec{l}_i^{\,T}(s)\mathbf{M}(s) = \vec{l}_i^{\,T}(s)\mathbf{M}(s)$ such that $\vec{l}_i^{\,T}(s)\vec{r}_j(s) = \delta_{i,j}$. Ideal adiabatic dynamics may be defined as that for which the dynamical coefficients of the instantaneous eigenvectors decouple. In a parallel transported eigenbasis, i.e., $\vec{l}_i^{\,T}(s)\vec{r}_i'(s) = 0$, where the prime denotes the derivative with respect to s, the adiabatic solution, or adiabatic prediction, is

$$\mathcal{U}_{i,j}(t) = \delta_{i,j}, \tag{A3}$$

where we have expanded the evolution operator $\mathcal{U}$ thus

$$\mathcal{U}(t) = \sum_{i,j} \mathcal{U}_{i,j} \exp\left(-iT \int_0^s ds' \lambda_i(s')\right) \vec{r}_i(s) \vec{l}_j^{\,T}(0). \quad \text{(A4)}$$

In the adiabatic solution the interaction between the dynamical coefficients of the instantaneous eigenvectors due to the finite variation of these eigenvectors is ignored. The full equation of motion for $\mathcal{U}$ expanded as above is

$$\dot{\mathcal{U}}_{p,q} = -i \sum_{i \neq p} T^{-1} \tilde{f}_{p,i}(s) \times \exp\left(-iT \int_0^s ds' [\lambda_i(s') - \lambda_p(s')]\right) \mathcal{U}_{i,p}, \quad \text{(A5)}$$

where we have defined

$$\tilde{f}_{p,i}(s) := -i \vec{l}_p^{\,T}(s) \vec{r}\,'_i(s). \quad \text{(A6)}$$

The adiabatic solution ignores $\tilde{f}_{p,q}(s)$ for $p \neq q$. Assuming the system to be initialized to the instantaneous eigenvector q, first-order perturbation theory yields that the solution for the coefficient x_p of the instantaneous eigenvector p where $p \neq q$ is

$$x_p(t) \simeq \frac{T^{-1} \tilde{f}_{p,q}(s) \exp\left(-iT \int_0^s ds' [\lambda_q(s') - \lambda_p(s')]\right)}{\lambda_q(s) - \lambda_p(s)}. \quad \text{(A7)}$$

This expression vanishes linearly with $|T^{-1}/[\lambda_q(s) - \lambda_p(s)]|$ but diverges exponentially with $T \operatorname{Im} \int_0^s ds' [\lambda_q(s') - \lambda_p(s')]$ if $\operatorname{Im} \int_0^s ds' \lambda_q(s') > \operatorname{Im} \int_0^s ds' \lambda_p(s')$. Second-order perturbation theory contains no more information as regards x_p but does reveal that $x_q(t)$ differs from unity with an analogous scaling. The traditional quantum adiabatic condition

$$\varepsilon_{p,q}(t) := \left| \frac{T^{-1} \tilde{f}_{p,q}(s)}{\lambda_q(s) - \lambda_p(s)} \right| \ll 1 \quad \text{(A8)}$$

and therefore only ensures adiabaticity for those elements of $\mathcal{U}$ for which $\operatorname{Im} \int_0^s ds' \lambda_i(s')$ is greatest, i.e., the least dissipative instantaneous eigenvectors. It obviously cannot be the case that every eigenvector is least dissipative, unless all are degenerate, and it is therefore impossible that the adiabatic solution (A3) holds. In the context of non-Hermitian systems it therefore seems pertinent to call Eq. (A8) the quasiadiabatic condition. So long as we initialize to the least dissipative instantaneous eigenstate and so long as this eigenstate remains the least dissipative, the quasiadiabatic condition ensures adiabaticity. However, if we initialize to an eigenstate that is not the least dissipative, or the quality of being least dissipative is exchanged, then perturbation theory breaks down.

2. Relative nonadiabatic transition amplitudes as a slow-fast system

In the main text we argued that for our two-dimensional case the simplest encompassing dynamical description of adiabaticity is afforded by the relative nonadiabatic transition amplitudes, the ratios of the elements of the evolution operator expressed in a parallel transported eigenbasis. Let us recall the equation of motion for the relative nonadiabatic transition amplitude $R(t)$ as defined in the paper:

$$\dot{R} = -2i\lambda(s)R - iT^{-1}\tilde{f}(s)(1 + R^2). \quad \text{(A9)}$$

Treating λ and $\tilde{f}$ as dynamical variables themselves, in the limit $T^{-1} \to 0$ this becomes

$$\dot{R} = -2i\lambda(s_0)R - iT^{-1}\tilde{f}(s_0)(1 + R^2), \quad \text{(A10)}$$

where $s_0 = T^{-1}t_0$ and t_0 is the initial time. On the other hand, we may rewrite the equation of motion using s as the independent variable

$$T^{-1}R' = -2i\lambda(s)R - iT^{-1}\tilde{f}(s)(1 + R^2), \quad \text{(A11)}$$

whereupon similarly taking $T^{-1} \to 0$ yields

$$0 = -2i\lambda(s)R - iT^{-1}\tilde{f}(s)(1 + R^2). \quad \text{(A12)}$$

The difference between Eqs. (A10) and (A12) is that the former is over a time scale of order T^{-1} and is hence fast, while the latter is over a time scale of order 1 and is hence slow; we have a slow-fast system. Furthermore, we notice here that the fast time-scale equation is differential and the slow algebraic. This is often taken as the definition of a singularly perturbed system and it means that any perturbative approach in T^{-1} can only be valid for times of order T^{-1}. In order to study the long-time behavior we must turn to a nonstandard analysis.

3. Slow manifolds

The solutions of the slow time scale (A12) are the fixed points of the fast time scale (A10) and as such are known as instantaneous fixed points. We recall their approximate expressions from the main text:

$$R^{\mathrm{ad}}(s) \simeq -\frac{T^{-1}\tilde{f}(s)}{2\lambda(s)}, \qquad R^{\mathrm{nad}}(s) \simeq -\frac{2\lambda(s)}{T^{-1}\tilde{f}(s)}. \quad \text{(A13)}$$

Since these are the fixed points of Eq. (A10) we may use Eq. (A10) to perform a stability analysis. One finds that $R^{\mathrm{ad}}(s)$ is stable if and only if $\operatorname{Im}\lambda(s) < 0$, while $R^{\mathrm{nad}}(s)$ is stable if and only if $\operatorname{Im}\lambda(s) > 0$, and the possible local phase portraits are stable star, stable spiral, center, unstable spiral, and unstable star [52]. Evidently, the only possible bifurcation is from a stable spiral to an unstable spiral through a center. The locus of points $R^{\mathrm{ad}}(s)$ over s is called a slow manifold and is defined as $M^{\mathrm{ad}} = \{R^{\mathrm{ad}}(s) : s\}$, and similarly for $R^{\mathrm{nad}}(s)$.

4. Adiabatic manifolds

Due to finite variations in $\lambda(s)$ and $\tilde{f}(s)$, the slow manifolds M^{ad} and M^{nad} are in fact not locally invariant. Nevertheless, a theorem due to Fenichel [53] ensures the existence of locally invariant manifolds in a T^{-1} neighborhood of M^{ad} and M^{nad}. These locally invariant manifolds are called adiabatic manifolds and are denoted by $\mathcal{M}^{\mathrm{ad}}$ and $\mathcal{M}^{\mathrm{nad}}$, respectively. The adiabatic manifolds do not obey a simple equation of motion, but we may find a good approximation by considering the particular integral of the N-times linearized equation of motion. We focus on $\mathcal{M}^{\mathrm{ad}}$ for clarity. Following the argument

of example 2.1.10 in Ref. [33], one arrives at $\mathcal{M}^{\rm ad} = \{\mathcal{R}^{\rm ad}(s) : s\}$, where

$$\mathcal{R}^{\rm ad}(s) \simeq \sum_{n=0}^{N-1} T^{-n} \left(\frac{-1}{2i\lambda(s)}\frac{d}{ds}\right)^n R^{\rm ad}(s) \tag{A14}$$

and N is an optimal truncation with a remainder of order $e^{-C/T^{-1}}$ for some $C > 0$. The expression for $\mathcal{R}^{\rm nad}(s)$ is analogous. We describe $\mathcal{R}^{\rm ad}(s)$ and $\mathcal{R}^{\rm nad}(s)$ as attractive or unattractive analogously to $R^{\rm ad}(s)$ and $R^{\rm nad}(s)$ being stable or unstable, respectively.

5. Stability loss delay

At certain critical times t_*, or s_*, the stability of the instantaneous fixed points swaps. For example, $R^{\rm ad}(s)$ becomes unstable and $R^{\rm nad}(s)$ becomes stable at $s = s_*$ such that $\mathrm{Im}\lambda(s_*) = 0$ and $\mathrm{Im}\lambda'(s_*) > 0$. One might naively suppose an immediate transition between $M^{\rm ad}$ and $M^{\rm nad}$ at $s = s_*$, but this is not the case. The bifurcation is dynamical and the type is degenerate Hopf, which in general exhibits the phenomenon known as stability loss delay: The solution $R(t)$ continues to follow, say, $R^{\rm ad}(s)$ for a significant time past its loss of stability. Following the argument in Sec. 2 of Ref. [51], one finds that away from $s = s_*$ the solution has the asymptotic expansion

$$R(t) \sim Ae^{\tilde{\Psi}(s)/T^{-1}} + \mathcal{R}^{\rm ad}(s), \tag{A15}$$

where

$$\tilde{\Psi}(s) = -2i\int_{s_*}^{s} ds'\lambda(s'), \tag{A16}$$

while at $s = s_*$ the solution exhibits the discontinuity

$$\Delta = -i\int_{s_-^*}^{s_+^*} ds\,\tilde{f}(s)e^{-\tilde{\Psi}(s)/T^{-1}}, \tag{A17}$$

where $s_-^* < s_*$ and $s_+^* > s_*$ are the intersections of the level curve of $\mathrm{Re}\Psi$ that includes the point $z_* \in \mathbb{C}$ such that $\lambda(z_*) = 0$. In order to incorporate this discontinuity in the asymptotic expansion of the solution for $R(t)$ we add the term $\Theta(s - s_*)\Delta e^{\tilde{\Psi}(s)/T^{-1}}$, where Θ is the Heaviside step function. This term is proportional to $e^{[\tilde{\Psi}(s)-\tilde{\Psi}(z_*)]/T^{-1}}$ and therefore diverges as $T^{-1} \to 0$ for any time t such that $\mathrm{Re}\tilde{\Psi}(s) - \mathrm{Re}\tilde{\Psi}(z_*) > 0$. Thus, the times $t_-^* < t_*$ and $t_+^* > t_*$ corresponding to s_-^* and s_+^* are such that (i) if the solution enters a neighborhood of $M^{\rm ad}$ before t_-^* then it must leave at t_+^*, (ii) if the solution enters a neighborhood of $M^{\rm ad}$ after t_-^* at $t_- < t_*$ then it must leave at $t_+ > t_*$ such that $\mathrm{Re}\tilde{\Psi}(s_+) - \mathrm{Re}\tilde{\Psi}(s_-) = 0$, and (iii) if the solution leaves a neighborhood of $M^{\rm ad}$ after t_+^* then it must have entered at t_-^*. Since the third case is sure to be rare, one typically calls t_+^* the maximal delay time. Note that this maximal delay time is precisely the quasiadiabatic limit of the delay time t_+ calculated via Eq. (26).

For an analytic example of a maximal delay time, let us consider the path analyzed in Sec. III B. In this case the level curves of $\mathrm{Re}\tilde{\Psi}$ are

$$e^{-\pi\,\mathrm{Im}z}\cos(\pi\,\mathrm{Re}z) \simeq \text{const.} \tag{A18}$$

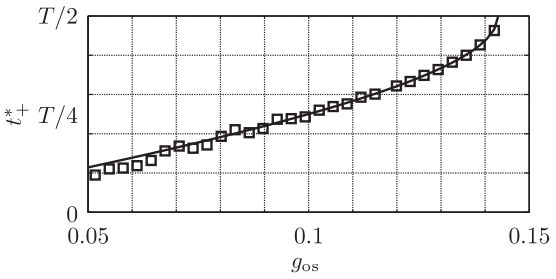

FIG. 8. Plot of the theoretical maximal delay time (solid line) and numerically observed departure times from a 5% neighborhood of $R^{\rm ad}(s)$ (open squares) for case (c) from Sec. III E.

Evidently, any $s_- < 0$ such that $s_- > -1/2$ is connected to $s_+ = -s_- > 0$ by these level curves. The maximal delay time is therefore $t_+^* = T/2$, which agrees with the main text.

For a numerical example, let us consider case (c) from Sec. III E. Here we calculate the theoretical maximal delay time by numerically finding the complex root of $\lambda(z)$, i.e., z_*, and then numerically finding where the level curve of $\mathrm{Re}\tilde{\Psi}$ on which z_* lies intersects the real axis. The results are plotted in Fig. 8. Also plotted in the figure are the results of a numerical solution where we have initialized to a neighborhood of $R^{\rm ad}(s)$ at $s = s_-^*$ and asked for when the numerical solution departs from this neighborhood. The agreement between the theoretical maximal delay time and the numerically observed departure time is very good. Furthermore, we see qualitatively the same results as those shown in Fig. 6; the quantitative difference is simply due to the finite time required for $R(t)$ to leave a small neighborhood of $M^{\rm ad}$ and reach $|R(t)| = 1$.

APPENDIX B: NONADIABATIC TRANSITIONS AS A MANIFESTATION OF THE STOKES PHENOMENON OF ASYMPTOTICS

The Stokes phenomenon of asymptotics is that subdominant exponentials in the asymptotic expansion of certain functions disappear and reappear in different sections of the complex plane with different coefficients. In Stokes's words [54], "...the inferior term enters as it were into the mist, is hidden for a little while from view, and comes out with its coefficient changed." Berry and Uzdin [26] uncovered the presence of the Stokes phenomenon of asymptotics in the solutions of specific exactly solvable models of quasiadiabatic non-Hermitian systems and identify nonadiabatic transitions in such systems as a manifestation. In this appendix we review one such example.

Let us consider again the parametrization studied in Sec. III B: $\omega(t) = r\sin\phi(t)$, $\gamma(t) = 1$, and $g(t) = 1/2 + r\cos\phi(t)$ with $r \ll 1$ and $\dot{\phi}(t) = \dot{\phi} = 2\pi/T = \text{const}$. An exact solution for this example is presented by Berry [31], which we now review. Constructing the analogous quantity to R in the circular basis

$$\vec{r}_{\circlearrowleft} = \frac{1}{\sqrt{2}}\begin{pmatrix}1\\ i\end{pmatrix}, \quad \vec{r}_{\circlearrowright} = \frac{1}{\sqrt{2}}\begin{pmatrix}1\\ -i\end{pmatrix}, \tag{B1}$$

which we denote by p, i.e., $\vec{x}(t) = c_{\circlearrowleft}(t)\vec{r}_{\circlearrowleft} + c_{\circlearrowright}(t)\vec{r}_{\circlearrowright}$ and $p(t) = c_{\circlearrowright}(t)/c_{\circlearrowleft}(t)$, one arrives at the equation of motion

$$\dot{p} \simeq re^{i\phi(t)} + p^2, \tag{B2}$$

where we have used $r \ll 1$. Note that $\vec{r}_{\circlearrowleft}$ and $\vec{r}_{\circlearrowright}$ are not eigenvectors. Introducing the new independent variable $\zeta = (i/2)(2\varepsilon)^{-1}e^{i\phi(t)/2}$, where $\varepsilon = \pi/4\sqrt{r}T$, and using the ansatz $p(t) = -(d/dt)\log f(\zeta)$ yields

$$\zeta^2\frac{d^2f}{d\zeta^2} + \zeta\frac{df}{d\zeta} + \zeta^2 f = 0. \tag{B3}$$

This is the zeroth-order Bessel equation and the solution from time $t = t_0$ is thus

$$p(t) = \frac{i}{2}\dot{\phi}\zeta\frac{\mathcal{C}_1(\zeta)}{\mathcal{C}_0(\zeta)}, \tag{B4}$$

where $\mathcal{C}_n(\zeta) = c_J J_n(\zeta) + c_Y Y_n(\zeta)$ is a linear combination of order n Bessel functions of the first and second kinds with the ratio

$$\frac{c_Y}{c_J} = -\frac{2ip(t_0)J_0(\zeta_0) + \dot{\phi}\zeta_0 J_1(\zeta_0)}{2ip(t_0)Y_0(\zeta_0) + \dot{\phi}\zeta_0 Y_1(\zeta_0)}, \tag{B5}$$

where $p(t_0)$ is the initial condition for p and $\zeta_0 = (i/2)(2\varepsilon)^{-1}e^{i\phi(t_0)/2}$.

In order to translate this result into an expression for $R(t)$ we have only to transform from the circular basis (B1) to the original basis and then from that to the parallel transported eigenbasis (5),

$$\vec{r}_-(t) = \begin{pmatrix}\cos\vartheta(t)/2\\ \sin\vartheta(t)/2\end{pmatrix}, \quad \vec{r}_+(t) = \begin{pmatrix}-\sin\vartheta(t)/2\\ \cos\vartheta(t)/2\end{pmatrix}, \tag{B6}$$

where $\tan\vartheta(t) = -g(t)/[\omega(t) + i\gamma(t)/2]$. Recognizing the effect of such transformations on p and R as Möbius transformations, it is immediately seen that

$$p(t_0) = e^{i\vartheta(t_0)}\frac{1 + iR(t_0)}{1 - iR(t_0)}, \tag{B7}$$

where $R(t_0)$ is the initial condition for R, and

$$R(t) = i\frac{1 - e^{-i\vartheta(t)}p(t)}{1 + e^{-i\vartheta(t)}p(t)}. \tag{B8}$$

Let us focus on the asymptotic expansion about $t = t_*$ where $R^{\mathrm{ad}}(t)$ becomes unstable. Recalling that $\lambda(t) \simeq \sqrt{r}e^{i\phi(t)/2}$ and $\mathrm{Im}\lambda(t_*) = 0$, we see that with $\zeta_* = (i/2)(2\varepsilon)^{-1}e^{i\phi(t_*)/2}$ we have $\mathrm{Re}\zeta_* = 0$. Without loss of generality, we suppose $\mathrm{Im}\zeta_* > 0$. Using 9.1.35, 9.1.36, 9.2.1, and 9.2.2 in Ref. [47] and assuming that the solution is exponentially close to $R^{\mathrm{ad}}(t)$ by $t = t_*$ yields

$$R(t) \sim i\frac{1 - e^{\vartheta(t)}p^{\mathrm{ad}}(t) + 2i\Theta(-\mathrm{Re}\zeta)e^{2i\zeta}[1 - e^{\vartheta(t)}p^{\mathrm{nad}}(t)]}{1 + e^{\vartheta(t)}p^{\mathrm{ad}}(t) + 2i\Theta(-\mathrm{Re}\zeta)e^{2i\zeta}[1 + e^{\vartheta(t)}p^{\mathrm{nad}}(t)]} \tag{B9}$$

for $-\pi/2 < \arg\zeta < 3\pi/2$, where $p^{\mathrm{ad}}(t)$ and $p^{\mathrm{nad}}(t)$ correspond to $R^{\mathrm{ad}}(t)$ and $R^{\mathrm{nad}}(t)$, respectively, and Θ is the Heaviside step function. The discontinuity in this asymptotic expansion is precisely the Stokes phenomenon of asymptotics. For $t \in (t_* - T/2, t_* + T/2)$ the discontinuous term is subdominant and $R(t) \sim R^{\mathrm{ad}}(t)$, whereas for $t > t_* + T/2$ it is dominant and $R(t) \sim R^{\mathrm{nad}}(t)$. The connection to the expansion (16) from Sec. III B is more clearly seen by expanding to first order about $R^{\mathrm{ad}}(t)$:

$$R(t) \approx R^{\mathrm{ad}}(t) - 2\Theta(t - t_*)e^{-\exp[i\phi(t)/2]/2\varepsilon}. \tag{B10}$$

Comparing this expansion to Eq. (16), we find very good agreement. The small difference that here the discontinuity at $t = t_*$ is $\Delta = -2e^{-1/2\varepsilon}$ whereas in Sec. III D we found $\Delta = -\pi e^{-1/2\varepsilon}$ is principally due to the asymptotic expansions employed in calculating Eq. (B9), which differ from those used in calculating Eq. (16).

[1] M. Born, Z. Phys. A **40**, 167 (1927).
[2] S. G. Johnson, P. Bienstman, M. A. Skorobogatiy, M. Ibanescu, E. Lidorikis, and J. D. Joannopoulos, Phys. Rev. E **66**, 066608 (2002).
[3] E. Farhi, J. Goldstone, S. Gutmann, J. Lapan, A. Lundgren, and D. Preda, Science **292**, 472 (2001).
[4] T. Kato, *Perturbation Theory for Linear Operators*, 2nd ed. (Springer, Berlin, 1995).
[5] A. P. Seyranian and A. A. Mailybaev, *Multiparameter Stability Theory with Mechanical Applications* (World Scientific, Singapore, 2003).
[6] M. V. Berry, Czech. J. Phys. **54**, 1039 (2004).
[7] A. P. Seyranian, O. N. Kirillov, and A. A. Mailybaev, J. Phys. A: Math. Gen. **38**, 1723 (2005).
[8] I. Rotter, J. Phys. A: Math. Theor. **42**, 153001 (2009).
[9] N. Moiseyev, *Non-Hermitian Quantum Mechanics* (Cambridge University Press, Cambridge, 2011).
[10] W. D. Heiss, J. Phys. A: Math. Theor. **45**, 444016 (2012).
[11] D. C. Brody and E.-M. Graefe, Phys. Rev. Lett. **109**, 230405 (2012).
[12] N. Bachelard, C. Garay, J. Arlandis, R. Touzani, and P. Sebbah, arXiv:1407.8220.
[13] B. Peng, Ş. K. Özdemir, S. Rotter, H. Yilmaz, M. Liertzer, F. Monifi, C. M. Bender, F. Nori, and L. Yang, Science **346**, 328 (2014).
[14] P. Ambichl, K. G. Makris, L. Ge, Y. Chong, A. D. Stone, and S. Rotter, Phys. Rev. X **3**, 041030 (2013).
[15] S. Klaiman, U. Günther, and N. Moiseyev, Phys. Rev. Lett. **101**, 080402 (2008).
[16] C. E. Rüter, K. G. Makris, R. El-Ganeiny, D. N. Christodoulides, M. Segev, and D. Kip, Nat. Phys. **6**, 192 (2010).
[17] M. Brandstetter, M. Liertzer, C. Deutsch, P. Klang, J. Schöberl, H. E. Türeci, G. Strasser, K. Unterrainer, and S. Rotter, Nat. Commun. **5**, 4034 (2014).
[18] C. Dembowski, H.-D. Gräf, H. L. Harney, A. Heine, W. D. Heiss, H. Rehfeld, and A. Richter, Phys. Rev. Lett. **86**, 787 (2001).
[19] O. Latinne, N. J. Kylstra, M. Dörr, J. Purvis, M. Terau-Dunseath, C. J. Joachain, P. G. Burke, and C. J. Noble, Phys. Rev. Lett. **74**, 46 (1995).

[20] R. Lefebvre, O. Atabek, M. Šindelka, and N. Moiseyev, Phys. Rev. Lett **103**, 123003 (2009).
[21] O. Atabek, R. Lefebvre, M. Lepers, A. Jaouadi, O. Dulieu, and V. Kokoouline, Phys. Rev. Lett. **106**, 173002 (2011).
[22] A. Kvitsinsky and S. Putterman, J. Math. Phys. **32**, 1403 (1991).
[23] G. Nenciu and G. Rasche, J. Phys. A: Math. Gen. **25**, 5741 (1992).
[24] G. Dridi, S. Guérin, H. R. Jauslin, D. Viennot, and G. Jolicard, Phys. Rev. A **82**, 022109 (2010).
[25] R. Uzdin, A. Mailybaev, and N. Moiseyev, J. Phys. A: Math. Theor. **44**, 435302 (2011).
[26] M. V. Berry and R. Uzdin, J. Phys. A: Math. Theor. **44**, 435303 (2011).
[27] I. Gilary, A. A. Mailybaev, and N. Moiseyev, Phys. Rev. A **88**, 010102 (2013).
[28] A. Leclerc, G. Jolicard, and J. P. Killingbeck, J. Phys. B: At. Mol. Opt. **46**, 145503 (2013).
[29] E.-M. Graefe, A. A. Mailybaev, and N. Moiseyev, Phys. Rev. A **88**, 033842 (2013).
[30] D. Viennot, J. Phys. A: Math. Theor. **47**, 065302 (2014).
[31] M. V. Berry, J. Opt. **13**, 115701 (2011).
[32] M. V. Berry, Proc. R. Soc. London Ser. A **422**, 7 (1989).
[33] N. Berglund and B. Gentz, *Noise-Induced Phenomena in Slow-Fast Dynamical Systems: A Sample-Paths Approach* (Springer, London, 2006).
[34] M. Diener, Math. Intell. **6**, 38 (1984).
[35] A. I. Neishtadt, Discrete Cont. Dyn. Syst. **2**, 897 (2009).
[36] T. Gao, E. Estrecho, K. Y. Bliokh, T. C. H. Liew, M. D. Fraser, S. Brodbeck, M. Kamp, C. Schneider, S. Höfling, Y. Yamamoto, F. Nori, Y. S. Kivshar, A. G. Truscott, R. G. Dall, and E. A. Ostrovskaya, Nature **526**, 554 (2015).
[37] T. Faust, J. Rieger, M. J. Seitner, J. P. Kotthaus, and E. M. Weig, Nat. Phys. **9**, 485 (2013).
[38] H. Okamoto, A. Gourgout, C.-Y. Chang, K. Onomitsu, I. Mahboob, E. Y. Chang, and H. Yamaguchi, Nat. Phys. **9**, 480 (2013).
[39] X.-W. Xu, Y. Liu, C.-P. Sun, and Y. Li, Phys. Rev. A **92**, 013852 (2015).
[40] A. B. Shkarin, N. E. Flowers-Jacobs, S. W. Hoch, A. D. Kashkanova, C. Deutsch, J. Reichel, and J. G. E. Harris, Phys. Rev. Lett. **112**, 013602 (2014).
[41] H. Jing, S. K. Özdemir, X.-Y. Lü, J. Zhang, L. Yang, and F. Nori, Phys. Rev. Lett. **113**, 053604 (2014).
[42] R. Uzdin and M. Moiseyev, Phys. Rev. A **85**, 031804 (2012).
[43] J. Doppler *et al.* (unpublished).
[44] A. Leclerc, D. Viennot, and G. Jolicard, J. Phys. A: Math. Theor. **45**, 415201 (2012).
[45] S. Ibáñez and J. G. Muga, Phys. Rev. A **89**, 033403 (2014).
[46] I. S. Gradshteyn and I. M. Ryzhik, in *Table of Integrals, Series, and Products*, 7th ed., edited by A. Jeffrey and D. Zwillinger (Elsevier, London, 2007).
[47] M. Abramowitz and I. A. Stegun, *Handbook of Mathematical Functions With Formulas, Graphs, and Mathematical Tables* (Dover, New York, 1972).
[48] A. Bohun, M.Sc. thesis, Imperial College, 2011.
[49] A. I. Neishtadt, Diff. Equat. **23**, 1385 (1987).
[50] A. I. Neishtadt, Diff. Equat. **24**, 171 (1988).
[51] F. Diener and M. Diener, *Dynamical Bifurcations* (Springer, Berlin, 1991).
[52] P. Glendinning, *Stability, Instability and Chaos: An Introduction to the Theory of Nonlinear Differential Equations* (Cambridge University Press, Cambridge, 1994).
[53] N. Fenichel, J. Differ. Equations **31**, 53 (1979).
[54] G. G. Stokes, Acta Math. **26**, 393 (1902).